AD_____

Award Number:
W81XWH-07-1-0159

TITLE:
Identification and Therapeutic Targeting of Paracrine Senescence Factors in the Prostate Tumor Microenvironment

PRINCIPAL INVESTIGATOR:
James Dean, MD, PhD

CONTRACTING ORGANIZATION:
Fred Hutchinson Cancer Research Center
Seattle, WA 98109

REPORT DATE:
March 2009

TYPE OF REPORT:
Annual

PREPARED FOR: U.S. Army Medical Research and Materiel Command
Fort Detrick, Maryland 21702-5012

REPORT DOCUMENTATION PAGE

Form Approved
OMB No. 0704-0188

1. REPORT DATE *(DD-MM-YYYY)*	2. REPORT TYPE	3. DATES COVERED *(From - To)*
01-03-2009	Annual	1 Mar 2008 - 28 Feb 2009

4. TITLE AND SUBTITLE

Identification and Therapeutic Targeting of Paracrine Senescence Factors in the Prostate Tumor Microenvironment

5a. CONTRACT NUMBER

5b. GRANT NUMBER
W81XWH-07-1-0159

5c. PROGRAM ELEMENT NUMBER

6. AUTHOR(S)

James Dean, MD, PhD

5d. PROJECT NUMBER

5e. TASK NUMBER

5f. WORK UNIT NUMBER

7. PERFORMING ORGANIZATION NAME(S) AND ADDRESS(ES)

Fred Hutchinson Cancer
Research Center

Seattle, WA 98109

8. PERFORMING ORGANIZATION REPORT NUMBER

9. SPONSORING / MONITORING AGENCY NAME(S) AND ADDRESS(ES)
U.S. Army Medical Research
And Materiel Command
Fort Detrick, MD 21702-5012

10. SPONSOR/MONITOR'S ACRONYM(S)

11. SPONSOR/MONITOR'S REPORT NUMBER(S)

12. DISTRIBUTION / AVAILABILITY STATEMENT

Approved for public release; distribution unlimited

13. SUPPLEMENTARY NOTES

14. ABSTRACT
The Purpose of this proposal is to examine how senescence in the prostate may be caused by medical treatments for prostate cancer, and to identify senescence-associated factors which may mediate resistance of neoplastic epithelium. The effects of standard and targeted therapeutics on senescence-mediated resistance will be determined. To date, our major findings present a mixed picture of chemotherapy-induced senescence. Senescence-associated β-galactosidase staining has not identified significant chemotherapy-induced senescence, but quantitation of gene expression changes reveal a pervasive pattern of senescence changes. Correlation of chronological aging and senescence is seen. Detailed investigations into a putative secreted marker of senescence, STC1 find significant decreases in cancer compared to benign prostate glands and possible links to hepatocyte growth factor in the prostate microenvironment. Finally, our clinical trial of neoadjuvant anti-IGF-1R antibody therapy with combined androgen deprivation prior to prostatectomy will examine the clinical effects of abrogating a pathway which is altered in senescence.

15. SUBJECT TERMS
prostate, cancer, senescence, paracrine, resistance, chemotherapy, androgen deprivation

16. SECURITY CLASSIFICATION OF:			17. LIMITATION OF ABSTRACT	18. NUMBER OF PAGES	19a. NAME OF RESPONSIBLE PERSON
a. REPORT	b. ABSTRACT	c. THIS PAGE			19b. TELEPHONE NUMBER *(include area code)*
U	U	U	UU	27	UWAMRMC

Table of Contents

Introduction

Deaths due to prostate cancer- the second leading cause of cancer death in men in the United States - could be prevented with more effective treatments. Overcoming tumor cell resistance to the effects of androgen deprivation and chemotherapies would significantly improve the morbidity and mortality of prostate cancer. We ***hypothesize*** that the induction of cellular senescence in the tumor microenvironment by androgen deprivation and cytotoxic chemotherapy promotes the resistance and survival of carcinoma cells. We further ***hypothesize*** that targeting senescence-associated pro-survival paracrine factors will enhance the effects of these therapies and enhance response rates.

To address these hypotheses, we have three aims: First, to identify senescence changes in prostate tissue induced by androgen deprivation and chemotherapy, specifically focusing on identifying factors with the potential to influence the survival/resistance of neoplastic epithelium via paracrine mechanisms. Second, to evaluate the effects of inhibiting specific senescence-associated pro-survival factors using *in vivo* models. Third, to develop and execute clinical trials designed to inhibit senescence-associated paracrine survival mechanisms and determine if enhanced tumor responses can be achieved.

Body

The following summarizes the research accomplishments of the first year of this proposal, as associated with each task in the Statement of Work.

Technical Objective 1: To determine the effects of chemotherapy and androgen ablation therapy on the frequency, type, and location of senescent cells in the prostate, and to identify changes in levels of senescenc-associated signaling molecules found in those tissues.

Objective 1a. *Identify senescent cells in pre- and post-chemotherapy prostate tissues from 58 patients.*

Task 1. Perform histochemical staining of a defined set of senescence biomarkers. (Months 1-6) As previously described, histochemical staining for the "gold standard" marker of senescence, the Senescence-Associated β-Galactosidase (SA-β-Gal) on post-chemotherapy prostate tissues from a random sample of 25 treated patients yielded highly variable results in an optimized assay with positive staining only noted in 6 of the patients. Given these results, it was our judgement that analyses of pre-treatment biopsy tissues were not likely to yield useful data with this method. The p16(INK4a) and DcR2 markers of senescence were also evaluated using Tissue Microarray of Aging and Prostate Cancer.

To compare staining pre- and post-treatment samples, it is necessary to be able to stain frozen tissues, as the pre-treatment biopsy cores obtained for research purposes in this study of neoadjuvant chemotherapy were preserved in this fashion to allow gene expression analysis, and not fixed and embedded in the standard fashion. Given our interest in modulating possible signaling pathways in senescence and the limited amount of tissue available for staining analyses, further staining to identify senescent cells was deferred in this interim to allow optimization and staining of the secreted signaling molecule STC1.

Task 2. Analyze stained tissues, quantitating frequency of positive staining cells in the epithelium versus stroma, in or near benign versus neoplastic prostate glands. (Months 2-8) Prior work demonstrated low levels of staining for p16(INK4A) in the benign epithelium and stroma. In the benign epithelium, approximately 1-3% of the cells had identifiable staining, assuming average staining level of 1+. In the stroma a similar number of cells, approximately 1-2% of cells stained positively for p16. In both compartments, there was an identifiable increase that occurred with aging, but obviously, these cells still represented rare events. By contrast, many more cells in the neoplastic epithelium stained for p16 (about 30%), but there was no change seen with aging.

In comparison, the DcR2 biomarker of aging also stained very few cells in the stroma (0.2-0.7%). With aging, there was a significant increase in these still rarely staining cells. In the neoplastic epithelium, there were very high numbers of cells with positive staining, representing 88-97% of cells. There was no increase with aging. Only in the benign epithelium was there a significant increase in DcR2 staining seen with aging, that occurred in a significant fraction of the cells evaluated. In the young cohort, 16.5% of cells stained positively, compared to 39% of cells in the aged cohort.

Task 3. Perform statistical analyses to determine the significance of staining differences between the various compartments and differences before and after chemotherapy. (Months 2-8) As previously described, and as detailed above, there were statistically significant increases in staining of benign epithelium and stromal compartments in aged men, when compared to young men. However, close evaluation of this staining reveal that only DcR2 staining of the benign epithelium was notable for a reasonable frequency of staining in combination with this statistically significant increase. Based on this, and given the limited number and amount of tissues available for these analyses, DcR2 staining will be further evaluated as a senescence marker in these tissues.

Objective 1b. *Identify senescent cells in pre- and post-androgen ablation prostate tissues from 48 patients.*

Task 4. Perform histochemical staining of a defined set of senescence biomarkers. (Months 12-20) - pending To date, 31 patients have been enrolled, and 28 have been treated on this protocol of neoadjuvant androgen ablation therapy given prior to prostatectomy. In order to ensure optimal results in analyses of these limited tissues, we have opted to defer staining of these tissues to synchronize with other analyses, and to allow choice of stain.

Task 5. Analyze stained tissues, quantitating frequency of positive staining cells in the epithelium versus stroma, in or near benign versus neoplastic prostate glands. (Months 13-22)-pending

Task 6. Perform statistical analyses to determine the significance of staining differences between the various compartments and differences before and after chemotherapy. (Months 13-22)-pending

Objective 1c. *Examine senescence-associated signaling molecules in pre- and post-chemotherapy prostate tissues from 58 patients.*

Task 7. Perform histochemical staining of secreted signaling molecules. (Months 3-18)

Tissue Microarray of Aging: As with the p16 and DcR2 immunohistochemistry described above, we also employed the tissue microarray of aging and prostate cancer to optimize the staining for a set of senescence-associated, secreted signaling molecules as described previously. To date, we have completed staining and analyses for STC1, GDF15, CXCL1 and IL8.

Post-Chemotherapy Tissues: STC1 staining has been completed in a limited set of post-chemotherapy prostate tissues as per the above Objective 1c.

Consecutive Serial Section Immunostaining Co-localization: Given the interesting heterogeneity in stromal STC1 staining in the prostate observed in the Tissue Microarray of Aging experiments, we completed an experiment using consecutive serial sections of a neoplastic prostate gland, interspersing STC1-stained sections with staining for various other likely and interesting possible constituents of the stroma. These components included fibroblasts/myofibroblasts, endothelium, neurons, macrophages and dendritic cells. To address possible fibroblastic and myofibroblastic staining, TE7, Caldesmon, Sm-a-actin, and Factor XIIIa were stained. Neuronal staining was assayed with Neurofilament and S100. Dendritic markers included CD21, CD35 and CD1a. Endothelium was stained with CD31 and CD34. Macrophages were stained with CD68.

Rapid Autopsy Prostate Cancer Metastases Microarray: We also examined STC1 staining in a case series of bony metastases within a tissue microarray derived from patients who underwent a rapid autopsy for the purpose of collecting metastatic prostate cancer deposits. These patients had been exposed to a heterogeneous set of medical therapies for metastatic prostate cancer, including hormonal therapies and chemotherapies prior to their death. Thus, these tissues are a valuable resource for examining the combined effect of these therapies in patients with advanced disease. In particular, 44 bony metastases have been reviewed to date.

Task 8. Analyze stained tissues, quantitating staining intensities and locations of positive staining; epithelium versus stroma, in or near benign versus neoplastic prostate glands. (Months 4-20)

Tissue Microarray of Aging: As described previously, the staining patterns of STC1 and GDF15 have been analyzed similarly to the p16 and DcR2 analyses as described above. We quantitated the intensity and the frequency of staining in the benign epithelium, neoplastic epithelium, and the stroma, using a 0-2 point scale for staining intensity as with p16 and DcR2 analysis. An example of this staining is shown in Figure 1 for the purposes of comparison with subsequent studies. In the three sections shown, cells within Gleason Pattern 3 glands (arrow 1) nearly all show significant staining, with heterogeneity in staining intensity. Overall in the TMA, there was definitely a significant amount of variability to STC1 staining of neoplastic glands. Some glands showed virtually no staining, while others showed very intense STC1 staining. Presumably, this reflects the inherent variability in the genetic background of different neoplasms and/or variability in senescence changes in different cancers. By contrast, overall there was significantly more staining of STC1 in the benign epithelial glands. Although there was variability in the staining patterns, the overall patterns were either one of lower, 1+, staining seen consistently throughout the glands (arrows 2), or more focal and intense staining seen scattered in cells through the glands (arrow 3). This consistency is reflected in the approximately 50% increase in staining scores, reflecting the average amount of staining through each sample. Most intriguingly, there was a heterogeneity in stromal staining which was not as easily explained. Although fibroblastic and myofibroblastic stroma are presumed to comprise the majority of the stromal compartment, many other cell types may also be present permanently or transiently. In some cores, a more diffuse staining of the stroma can be appreciated (arrows 4), such as in the

top and bottom panels of Figure 1. In other cores, such as the middle panel of Figure 1, there are very intense, individual cells that can be appreciated. Of the intensely staining cells in the stroma, several patterns can also be appreciated in the stroma. In some cases, clusters of intensely staining cells also have the morphological features of nerve bundles (arrow 5). Other cells had a linear appearance, possibly consistent with nerves or myofibroblasts (arrow 6). Finally, scattered cells with intense staining were more non-descript and could not be identified morphologically.

Post-chemotherapy prostate tissues: As described in my original proposal, one goal of this project is to examine prostate tissues for changes in senescence-associated signaling molecules after chemotherapy treatments. We applied the optimized protocol for STC1, which demonstrated intriguing differences in staining of benign compared to neoplastic epithelium, as well as a borderline significance in stromal staining with aging, to stain a limited set of post-chemotherapy prostate tissues. A total of 10 patient samples were stained for STC1. As with the SA-B-Gal staining described above, flash-frozen sections were employed in this study. This was necessary to allow possible comparisons with pre-treatment tissues. Representative photos of two patient samples from this study are shown in Figures 2 and 3. In each case, two illustrative areas of STC1 staining were selected, with photos also taken of the corresponding area from these sections exposed to a non-immune antiserum as a negative control.

Figure 2, Panel A shows a homogeneous, lightly staining gland with little background in the negative control. The stroma also shows scattered cells staining intensely, in a background of diffuse staining. However, in the stroma, the negative control shows similar diffuse staining of the stroma, albeit at lower intensity. Intensely staining stromal cells have a similar decreased intensity in the negative control. Panel B shows a single, intensely staining linear array of cells having the appearance of a nerve bundle. The remainder of the stroma was as described for Panel A.

Figure 3, Panel A shows the intense and specific staining that is associated with cell bundles having the appearance of nerve bundles. Diffuse staining pattern and some other rare scattered intensely-staining cells can also be appreciated in the stroma, but comparison with the negative control shows that the staining in these areas is much more equivocal. By contrast with the formalin-fixed, paraffin-embedded (FFPE) tissues of the TMA of aging, much less staining of benign epithelial glands could be appreciated in these frozen sections with a significant background in the negative control. In Panel B, numerous neoplastic epithelial glands are stained rather intensely with STC1. Similar to the staining in the stroma and the benign epithelium, there is also a significant amount of background staining seen in the negative control.

Thus, staining can be appreciated in the stroma, benign epithelium and neoplastic epithelium of these post-chemotherapy treated patients. However, unlike the FFPE staining achieved in the TMA of aging, there is a significant amount of background staining in all three compartments, despite optimization of the protocol. In the future, additional optimization will be attempted in hopes of allowing further analyses changes of this very interesting molecule after chemotherapy treatment in the prostate.

Consecutive Serial Section Immunostaining Co-localization: As described above, we completed an experiment using consecutive serial sections of a neoplastic prostate gland, interspersing STC1-stained sections with staining for various other likely and interesting possible constituents of the stroma. No significant co-localization could be appreciated for dendritic markers including CD21, CD35 and CD1a, the macrophage marker CD68, the endothelial markers CD31 and CD34, or the fibroblastic/myofibroblastic markers TE7 and Factor XIIIa. By con-

trast, clear co-localization was demonstrated for the neuronal markers Neurofilament and S100, as well as the fibroblastic/myofibroblastic markers Caldesmon and Sm-a-actin.

Seen in Figures 4 and 5, the flanking STC1-stained sections are the top and bottom panels, with STC1-positive cell examples highlighted by the arrowheads. In the middle, staining for Caldesmon (Figure 4) and Sm-a-actin (Figure 5) is shown of intervening sections, with the similar cells also highlighted by the arrowheads. These data confirm the presumption that the majority of the stromal compartment is comprised of fibroblastic/myofibroblastic cells. Not surprisingly given their ubiquity, reasonable evidence is found for co-localization of STC1-staining cells with these two stains. This suggests that STC1 may be staining a minor sub-set of the fibroblastic stroma, perhaps the part which has undergone senescence. The lack of significant co-localization with the TE7 and Factor XIIIa staining is not surprising, as these markers are not ubiquitous through the stroma, but are only found to stain minor sub-sets of the stroma.

Staining of Neurofilament (Figure 6) and S100 (Figure 7) was even clear. Highly intense staining bundles of cells are seen in the STC1-stained panels at the top and bottom of each figure (arrows), while the intervening sections respectively stained for these neuronal markers co-localize with similarly intense staining of these cellular bundles. This even more unequivocally demonstrates that the nerves of the prostate are intensely stained with STC1 and retrospectively, identifies similar intensely-staining cell bundles in the TMA of aging and the post-chemotherapy tissues as almost certainly neuronal in origin. Other data, not shown, demonstrates that some of the intensely-staining linear cells as seen in the middle panel of Figure 1, are also likely neuronal in origin.

Rapid Autopsy Prostate Cancer Metastases Microarray: As described above, a tissue microarray consisting of various metastatic prostate cancer tissues obtained from men by rapid autopsy shortly after death was stained for STC1. 44 cores in this microarray are composed of bony metastases, with the balance including lymph nodes, kidney and liver samples. A representative set of interesting STC1 staining patterns of these bony metastases are shown in Figure 8. In panel A, several scattered metastatic prostate glands are interspersed into a sparsely cellular stroma adjacent to bone. In panel B, more intensely staining glands are interspersed with an extensive amount of bone. In panel C, intensely staining hematopoietic bone marrow is seen as an aggregate from the 7 o'clock to the 2 o'clock position, with interspersed fat globules. A more lightly staining ovoid composed of prostate glands is seen centered on the 3 o'clock position. In panel D, two deposits of metastatic prostate cancer are surrounded by a sparsely cellular stroma, with a small focus of more intensely staining hematopoietic bone marrow at the 11 o'clock position. These results are representative of the staining seen in the bone samples of this TMA, and suggest that the staining seen in the primary tumors is retained during the metastatic process. Analysis is ongoing and will include quantitative and qualitative comparisons of samples from different tissues of the same patients, as well as similar tissues across different patients. In this fashion, possible roles for STC1 in the metastatic processes may be suggested.

Exploratory investigations into mechanisms of STC1 function: Data has been published demonstrating that hepatocyte growth factor (HGF) is able to stimulate the secretion of STC1 from endothelial cells in vitro and was further correlated using a mouse model of ischemia (Zlot et al, 2003). We have previously shown that HGF secretion is increased by prostate stromal senescence in vitro (Bavik et al, 2006). Further, HGF is known to mediate pro-neoplastic processes in the prostate epithelium (Knudsen and Edlund, 2004). Thus, possible implication of STC1 as a modulator of HGF activity may shed light into its function in the prostate, as yet unknown.

Seen in Figure 9, STC1 secretion is increased by in vitro senescence of the prostate stromal cell line PSC27, compared to other proteins with unchanged (CST3, SPARC) or decreased (BMP1) secretion with senescence. Confluent PSC27 cells were next treated with recombinant HGF. Conditioned medium was collected after three days and STC1 levels were found to increased by HGF treatment (Figure 10, Left panel). To confirm the HGF pathway was active in these cells, the c-met protein was detected by Western blot of cell extracts treated for 15 minutes with HGF, and found to be present, albeit at much lower levels in PSC27 cells, compared to the PC3 positive control (Figure 10, Middle panel). Despite these low levels, however, the activated, phosphorylated form of c-met could be detected by Western Blot of the PSC27 cell extracts, in a similar fashion to the PC3 positive control. These data are intriguing and implicate STC1 as a potential modulator of HGF activity in the neoplastic prostate, in a similar fashion to STC1 modulation of HGF activity in the endothelium. One factor to note is that although much is known about the effects of HGF on prostate epithelium, little is known about its effects on the stroma. Certainly nothing is known about how STC1 might contribute to HGF activity in vivo, on the epithelium and on the stroma. Further experiments will elucidate the effects of HGF stimulation on senescent prostate stroma. Overexpression of STC1 will allow determination of its effects on HGF secretion and HGF effects. Neutralizing antibodies may be used to abgrogate HGF-induced STC1 secretion to examine HGF effects on prostate stroma separate from any STC1 effects. All together, these will certainly contribute to our understanding of HGF activity in the neoplastic prostate.

Task 9. Perform statistical analyses to determine the significance of staining differences between the various compartments and differences before and after chemotherapy. (Months 4-20) As described previously, statistical analyses demonstrated a statistically significant increase in GDF15 and decrease in STC1 staining of neoplastic epithelium compared to benign epithelium, but no significant changes in benign epithelium, neoplastic epithelium, or stroma in young men compared to older men. Further, no age-dependent change in the staining intensities, frequencies, or patterns could be discerned for the GDF15 and STC1 proteins. No significant stromal GDF15 staining was visualized. By contrast, the increased STC1 staining seen in the stroma bordered on the statistically significant ($p=0.09$). In fact, STC1 is the first protein we have examined with intense and widespread stromal staining patterns. Optimized protocols for IL8 and CXCL1 failed to yield staining that could be analyzed in a meaningful fashion.

Objective 1d. *Examine senescence-associated signaling molecules in pre- and post-androgen ablation prostate tissues from 48 patients.*

Task 10. Perform histochemical staining of secreted signaling molecules. (Months 12-36)-pending, see above.

Task 11. Analyze stained tissues, quantitating staining intensities and locations of positive staining; epithelium versus stroma, in or near benign versus neoplastic prostate glands. (Months 13-36)-pending

Task 12. Perform statistical analyses to determine the significance of staining differences between the various compartments and differences before and after chemotherapy. (Months 13-36)-pending

Objective 1e. *Correlate observed senescence staining results from Objectives 1a-1d with clinical outcomes and gene expression data.*

Task 13. Collate senescence staining results and clinical outcomes. (Months 4-40) - pending Attempts to identify a secreted senescence biomarker with altered levels due to therapeutic treatments are ongoing and critical to allow these correlative studies.

Task 14. Collaborate with Nelson laboratory members performing the parallel expression studies to correlate staining patterns with gene expression changes. (Months 4-40) - pending As described last year, we have performed quantitative real-time PCR experiments on RNA isolated from pre- and post-chemotherapy treated tissues. We demonstrated statistically significant increases in the expression of the senescence biomarkers p16 and p21 in all three compartments of the prostate, as a result of chemotherapy treatment

Technical Objective 2. To examine resistance of senescence-induced carcinogenesis and tumor progression to the effects of docetaxel and/or the anti-IGF-IR antibody IMC-A12 in a nude mouse xenoplant model.

Objective 2a. *Obtain regulatory approval for animal xenoplant trials.*

Task 15. Write animal protocol for therapy trials. (Months 1-2). This has been completed.

Task 16. Obtain necessary animal review board approval. (Months 2-5). Fred Hutchinson Cancer Research Center Institutional Animal Care and Use Committee approval has been obtained for the proposed studies (IACUC #1743). USAMRMC Animal Care and Use Review Office (ACURO) approval has also been obtained.

Objective 2b. *Determine the resistance of senescent-dependent carcinogenesis and early tumors to docetaxel chemotherapy.*

Task 17. Culture cells and prepare cellular recombinants with BPH1 or PC3 and primary prostate stromal cells, senescent, or not. Perform sub-kidney capsule implantation surgeries. After 2 weeks of recovery, treat mice with weekly docetaxel for 3 weeks. 2 months after completion of therapy, sacrifice mice and retrieve xenoplanted kidneys. (Months 5-12) - pending The experimental work proposed in this Objective, as with Objectives 2c and 2d continued to be largely deferred to allow commitment of time and energies into completion of the clinical trial described below in Objective 3a, Task 26, as well as the experimental studies described above. As described last year, we completed a series of studies designed to complement the therapy trials and have demonstrated that replicative senescence, as well as senescence induced by hydrogen peroxide, can mediate the growth stimulatory effects we previously described in our proposal. Technical issues with cell culture contamination have also been addressed during the last year, a vital pre-requisite to prevent infections of the grafted nude mice which will be used in these studies.

Task 18. Measure resulting graft sizes, fix and embed the tissues, then stain with Hematoxylin and Eosin and immunohistochemistry. Evaluate for invasiveness, senescent cell populations and neoplastic morphologies. (Months 8-14 - pending)

Task 19. Perform statistical analyses to determine significance of chemotherapy-induced changes in the senescent-stimulated, compared to the pre-senescent recombinants. (Months 10-16) - pending

Objective 2c. *Determine the effect of IMC-A12 on senescent-dependent carcinogenesis and early tumors.*

Task 20. Culture cells and prepare cellular recombinants with BPH1 or PC3 and primary prostate stromal cells, senescent, or not. Perform sub-kidney capsule implantation surgeries. After 2 weeks of recovery, treat mice with thrice weekly IMC-A12 injections continuously for 2 months, then sacrifice mice and dissect out kidneys. (Months 7-12) - pending. For further details please see explanation under Objective 2b, Task 17.

Task 21. Measure resulting graft sizes, fix and embed the tissues, then stain with Hematoxylin and Eosin and immunohistochemistry. Evaluate for invasiveness, senescent cell populations and neoplastic morphologies. (Months 10-14) - pending

Task 22. Perform statistical analyses to determine significance of chemotherapy-induced changes in the senescent-stimulated, compared to the pre-senescent recombinants. (Months 12-18) - pending

Objective 2d. *Determine the senescence-dependent resistance of advanced tumors to docetaxel chemotherapy and its modulation by IMC-A12.*

Task 23. Culture cells and prepare cellular recombinants with BPH1 or PC3 and primary prostate stromal cells, senescent, or not. Perform sub-kidney capsule implantation surgeries. Two months after implantation, treat mice with weekly docetaxel for 3 weeks, with or without IMC-A12 thrice weekly treatments. 3 weeks after completion of therapy, sacrifice mice and dissect out kidneys. (Months 10-18) - pending. For further details please see explanation under Objective 2b, Task 17.

Task 24. Measure resulting graft sizes, fix and embed the tissues, then stain with Hematoxylin and Eosin and immunohistochemistry. Evaluate for invasiveness, senescent cell populations and neoplastic morphologies. (Months 13-20 - pending)

Task 25. Perform statistical analyses to determine significance of chemotherapy-induced changes in the senescent-stimulated, compared to the pre-senescent recombinants. (Months 15-22) - pending

Technical Objective 3: To develop and execute clinical trials evaluating the effectiveness of inhibiting senescence-associated modulators of cancer cell survival in the treatment of prostate cancer. The lead candidate for such targeting is currently IGF1R in the insulin-like growth factor pathway. Other targets identified in Specific Aims/Technical Objectives 1 and 2 may also present opportunities for treatment of more novel targets. Optimal target selection and clinical trial design will be determined during year 2 of the proposal.

Objective 3a*: Participate in the execution and analysis of a Phase II clinical trial inhibiting senescence-associated modulators of cancer cell survival in combination with androgen ablation in the neoadjuvant setting prior to radical prostatectomy. The lead class of modulators are anti-IGF1R antibodies under development by Imclone (IMC-A12) or Pfizer (CP-751,871) which inhibit the insulin-like growth factor pathway. Other candidates/pathways will be considered and optimized during the clinical trial design phase of the project in year 2.*

Task 26. Design Clinical Trial (Months 15-18) As described in last year's annual report, I attended the 2007 ASCO/AACR Methods in Clinical Cancer Research workshop, July 27-August 3, 2007, during which time I had the opportunity to further refine the proposed clinical trial described above. Food and Drug Administration Investigational New Drug application had also been submitted and duly approved (IND 79729). During this reporting period, we obtained

approval of the University of Washington Human Subjects Review Committee V (institutional review board).

In this clinical trial, 28 patients will be treated with the Imclone anti-IGF-IR antibody IMC-A12 every two weeks simultaneously with combined androgen deprivation therapy (goserelin plus bicalutamide). After three months of this treatment, patients will undergo standard prostatectomy. Tissues excess to the needs of clinical pathological diagnosis and staging will be analyzed for several laboratory endpoints, including gene expression changes, and changes in cellular proteins by immunohistochemistry. All patients will have a pre-treatment prostate biopsy for the purposes of comparison with the prostatectomy tissues. The primary endpoint will be a pathological complete response rate predicted to be 20%. This will be compared to historical control data in which 5% of patients treated for 3 months with combined LHRH agonist and testosterone receptor antagonist prior to prostatectomy were found to have pathological complete response. This number of patients is calculated to provide 80% power with 5% one-sided Type I error rate.

Discussions with Ms. Johanna Kidwell of the Human Subjects Protection Office, Office of Research Protections at U.S. Army Medical Research and Material Command during this interim led to their requirement that I obtain local institutional review board approval and HSPO/ORP approval prior to my planned laboratory investigations into the senescence changes that may be detected in tissues from these patients.

Task 27. Develop recruitment materials, hold in-service for clinical providers and study coordinator. (Months 18-24) - pending. Recruitment materials were limited to internet postings on world-wide web sites for the Fred Hutchinson Cancer Research Center/University of Washington Cancer Consortium, University of Washington Health Sciences and the Fred Hutchinson Cancer Research Center web sites. In addition, the study was posted on clinicaltrials.gov as required.

In-service training sessions were presented to the infusion center nursing staff, familiarizing them with the scientific rationale of the treatment, goals of the study, and the practicalities of administration and monitoring for unexpected or serious adverse events. I have worked closely with the study coordinator in obtaining the IRB approvals. I also presented the clinical trial to physician providers and co-investigators.

Task 28. Recruit, enroll, and treat patients on study. Monitor and report adverse events. (Months 20-55) – pending

To date, 4 subjects have been enrolled and 3 subjects have completed treatment. There has been one complete response. There have been no serious or unexpected adverse events related to study treatment. No laboratory studies have been initiated to date.

Task 29. Analyze pre- and post-treatment tissues for changes senescent cell content and senescence-associated signaling molecule expression as described above (Objectives 1a. and 1c.). (Months 24-46) - pending

Task 30. Collate and analyze data. (Months 24-50) - pending

Objective 3b: *Design and execute a clinical trial combining docetaxel chemotherapy with an inhibitor of senescence-associated modulation of cancer cell survival in the neoadjuvant setting prior to radical prostatectomy. The anti-IGF1R antibodies such as IMC-A12 (Imclone) or CP-751,871 (Pfizer) are currently the lead candidates for inhibition. Other candidates/pathways will be considered and optimized during the clinical trial design phase of the project in year 3.*

Task 31. Write the protocol and required regulatory documents. (Months 24-30) - pending

Task 32. Obtain regulatory approval from Institutional Review Board. (Months 30-34) - pending

Task 33. Develop recruitment materials, hold in-service for clinical providers and study coordinator. (Months 34-36) - pending

Task 34. Recruit, enroll, and treat patients on study. Monitor and report adverse events. (Months 36-60) - pending

Task 35. Analyze pre- and post-treatment tissues for changes senescent cell content and senescence-associated signaling molecule expression as described above (Objectives 1a. and 1c.). (Months 40-55) - pending

Task 36. Collate and analyze data. (Months 34-60) - pending

Technical Objective 4: To complete data analyses, compile accomplishments and reportable outcomes, and write final project reports and manuscripts.

Objective 4a*: Prepare manuscript 1.*

Task 37. Describe changes in the extent and distribution of senescent cells in the prostate as a function of chemotherapy and androgen ablation therapies. Correlate with alterations in senescence-associated signaling molecules, gene expression studies and clinical outcome measures. (Months 38-44) - pending

Objective 4b: *Prepare manuscript 2.*

Task 38. Describe the effects of docetaxel, mitoxantrone, and IMC-A12 treatment on the nude mouse model of senescence-dependent carcinogenesis and progression. Inter-correlations of presence or absence of tumor, size of grafts, extent and distribution of senescent cells and levels of senescence-associated signaling molecules. (Months 24-30) - pending

Objective 4c*: Prepare manuscript 3.*

Task 39. Describe the clinical efficacy, side effect profile, and laboratory correlates data resulting from the combination of IMC-A12 with androgen ablation. (Months 50-60) - pending

Objective 4d*: Prepare manuscript 4.*

Task 40. Describe the clinical efficacy, side effect profile and laboratory correlate study results from the clinical trail combining IMC-A12 with chemotherapy. (Months 54-60) - pending

Key Research Accomplishments

• Based on staining conditions optimized using the TMA of aging as described in the last report, we stained a series of the post-chemotherapy-treated patient samples for STC1. To allow comparison with pre-treatment tissues, these were frozen, rather than FFPE samples. Unfortunately, despite further optimization for this type of sample, levels of background staining were seen which significantly limit our ability to interpret these results. There do appear to be staining of stroma, benign epithelium and neoplastic epithelium, but staining differences with and without

antibody are a matter of slight changes in intensity. Further analysis will be necessary to determine whether this staining can yield useful data.

• To better understand STC1 staining in the prostate and motivated by its intriguing and limited data in other organs and unknown role in the prostate, we performed an experiment staining serial prostate sections for various markers likely to be found in the stroma, including fibroblasts/myofibroblasts, dendritic cells, endothelium, macrophages, and neuronal cells. We have demonstrated co-localization of STC1-staining cells with the neuronal markers S100 and Neurofilament. We have also demonstrated co-localization of STC1 with the fibroblastic/myofibroblastic markers Caldesmon and Sm-a-actin. The neuronal staining appears to be uniform, suggesting high levels of STC1 expression irrespective of age or treatment status. By contrast, only a small fraction of the fibroblastic compartment stains for STC1, suggesting this may be a marker for altered or abnormal cells. Alternatively, STC1 may define a novel subset of the fibroblastic stroma of unknown signficance.

• We also stained a Tissue Microarray of Prostate Cancer Metastases. Analysis of bony metastases on this array demonstrates that STC1 staining is not lost, nor does it appear to be increased in association with metastasis in these patients with extensive histories of hormonal and chemotherapy treatments. Further analysis is ongoing and will address differences between patients for given metastasis sites, as well as differences with patients between different metastasis sites.

• Given the novel nature of STC1 as a previously undescribed moiety in the prostate, advantage has been taken to initiate preliminary experiments into possible mechanisms for its action in the prostate. This will greatly complement our immunohistochemical studies and may shed new light into HGF activity in the neoplastic prostate, a pathway currently under clinical development as a therapeutic target.

• Work on Objective 2 has been again been delayed to allow further work on Objectives 1 and 3, as well as to allow resolution of technical difficulties in the techniques required to allow the experiments planned for Objective 2. At this point, the technical issues with cell culture contamination have been resolved and work can move forward.

• We obtained IRB approvals for the clinical trial of Objective 3a, and in discussions with the HSPO/ORP/USAMMRMC, have clarified that HSPO oversight requires IRB approval for the laboratory studies I will undertake on the tissues from this clinical trial. This application is in process. To date, 4 patients have been enrolled on this trial of a planned 28 patients. Of the three patients who have undergone surgery, one complete response has been noted.

Reportable Outcomes

Publication:
Dean JP, Higano, CS. Does Chemotherapy Have a Role Before Hormone-Resistant Disease Develops? Current Urology Reports, In press. 2009.

Manuscript in Preparation:
Dean JP, Coleman I, Martin DB, Nelson, PS. Quantitative proteomic analysis of proteins released from prostate stromal cells with activation of the program of cellular senescence.

Conclusion

The research accomplished during this interim has more fully investigated STC1 as a novel biomarker of senescence and its potential contribution to prostate cancer, metastasis and response to treatment. We previously showed that STC1 was expressed at significantly higher levels in the benign epithelium, compared to the neoplastic epithelium. There was also an increase in stromal STC1 staining with aging which approached statistical significance. Further work examined STC1 staining of post-chemotherapy-treated tissues. Staining was identified in the benign, neoplastic and stromal compartments. Unfortunately, unexpected background staining in the negative controls limits our ability to interpret these results, particularly given the limited numbers of cases and amounts of tissue available for analysis. Under these limitations, it may not be possible to achieve statistical significance. We also examined STC1 staining of bony metastases from heavily pre-treated patients. In these patients, STC1 shows staining similar to that seen in untreated primary prostate tissues. Lack of changes in STC1 with metastasis and treatment may imply a lack of influence on these processes, or may simply reflect an ongoing process that is not affected by the change in microenvironment.

STC1 staining of the stromal compartment was more fully characterized, demonstrating uniform staining of neuronal cell bundles and individual neuronal cells in the prostate stroma. A small fraction of fibroblastic/myofibroblastic cells were also found to stain positively for STC1. Thus, STC1 staining may represent a fraction of these cells which have undergone senescence changes, a previously undefined compartment in the fibroblastic stroma, or both.

Finally, we have shown that STC1 secretion appears to be linked to HGF secretion in the prostate stromal cell model. It is unknown how the secretion of each factor may influence secretion and/or function of the other factor. Based of prior studies, it is possible that STC1 may modulate HGF activity in the stroma and/or the epithelium. This may be important to maintain stromal quiescence or senescence in the presence of HGF and other potentially pro-proliferative factors.

We have received regulatory approvals necessary to move forward in our clinical trial designed test how abrogation of the senescence-associated insulin-like growth factor signaling pathway can enhance the efficacy of standard combined androgen deprivation. Further institutional review board application to review proposed laboratory analyses of senescence changes is in process and will be duly submitted to HSPO/ORP/USAMMRMRC subsequent to approval.

As a result of the extensive work performed on the immunhistochemistry studies, the clinical trial, and technical cell culture issues, we continue to be behind our predicted timeline for the animal trials of the second specific aim. However, with resolution of these technical issues it is anticipated this work will move forward and results be available to support the immunohistochemical results.

As we continue to move forward, continuation of the work detailed for the first Technical Objective will more fully define the relationships of androgen deprivation therapy and chemotherapy with the induction of senescence in the prostate gland. Use of the in vivo mouse model of the effects of stromal senescence on prostate epithelial cells to examine how senescence changes may interfere with therapeutic efficacy. These data may provide the impetus and the insight necessary to allow us to ameliorate a potentially important source of resistance to medical therapies, optimizing outcomes for patients. Finally, the Phase II investigation of the insulin-like growth factor receptor antagonist IMC-A12 together with combined androgen deprivation therapy will start to test whether pathways of importance in senescence changes may also be important in cellular responses to standard medical therapies.

References

Bavik C, Coleman I, Dean JP, Knudsen B, Plymate S, and Nelson, PS, Cancer Research, 2006, 66(2)794-802.

Knudsen BS and Edlund M, Advances in Cancer Research, 2004, 91:31-67.

Zlot C, Ingle G, Hongo J, Yang S, Sheng Z, Schwall R, Paoni N, Wang F, Peale FV and Gerrisen ME, 2003, The Journal of Biological Chemistry, 278(48)47654-47659.

Appendices

none

Supporting Data

FIGURE 1. STC1 staining of prostate tissues from the TMA of aging.

A tissue microarray was stained for STC1 and detected with standard immunohistochemical methods. Three representative fields are shown.

FIGURE 2. STC1 staining of post-chemotherapy tissue KP-02.

STC1 staining as with Figure 1 was performed on the flash-frozen, post-chemotherapy treatment tissues from patient KP-02. Negative control composed of pre-immune serum instead of primary antibody is also shown.

FIGURE 3. STC1 staining of post-chemotherapy tissue KP-03.

STC1 staining as with Figure 1 was performed on the flash-frozen, post-chemotherapy treatment tissues from patient KP-03. Negative control composed of pre-immune serum instead of primary antibody is also shown.

FIGURE 4. Serial Section staining of STC1 and Caldesmon.

Consecutive serial sections obtained from a single neoplastic prostate gland were stained for STC1 as in Figure 1, as well as the standard pathological marker Caldesmon. The STC1-stained sections flank the Caldesmon-stained section.

FIGURE 5. Serial Section staining of STC1 and Sm-a-actin.

Consecutive serial sections obtained from a single neoplastic prostate gland were stained for STC1 as in Figure 1, as well as the standard pathological marker Sm-a-actin. The STC1-stained sections flank the Sm-a-actin-stained section.

FIGURE 6. Serial Section staining of STC1 and Neurofilament.

Consecutive serial sections obtained from a single neoplastic prostate gland were stained for STC1 as in Figure 1, as well as the standard pathological marker Neurofilament. The STC1-stained sections flank the Neurofilament-stained section.

FIGURE 7. Serial Section staining of STC1 and S100.

Consecutive serial sections obtained from a single neoplastic prostate gland were stained for STC1 as in Figure 1, as well as the standard pathological marker S100. The STC1-stained sections flank the S100-stained section.

FIGURE 8. STC1 staining of post-Chemo-Hormonally treated Bone Metastases.

Representative images were obtained from a tissue microarray comprised of tissue cores obtained from patients who underwent rapid autopsy. STC1 staining was as in Figure 1.

FIGURE 9. Western Blot of STC1, CST3, SPARC and BMP1 from Senescent prostate stroma.

The indicated primary antibody and appropriate secondary antibody were used to quantitate levels of the indicated protein in the concentrated conditioned medium from cells induced to become senescent, or not, and detected with chemoluminescence.

FIGURE 10. HGF effects on STC1 secretion, c-met levels and phosphorylation of c-met.

The indicated primary antibody and appropriate secondary antibody were used to quantitate levels of the indicated protein in the concentrated conditioned medium (STC1) or cell extracts (c-met and phospho-c-met) from cells treated with HGF or not.

Figure 1.

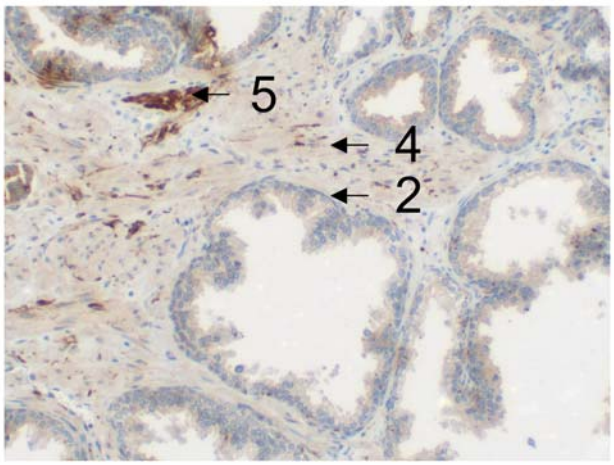

Benign Epithelium and Stroma

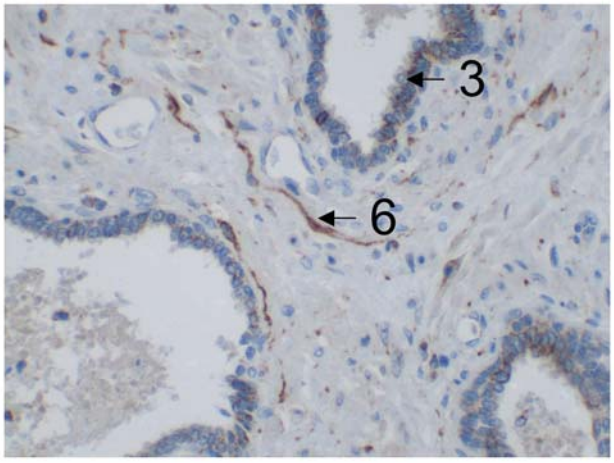

Benign Epithelium and Stroma

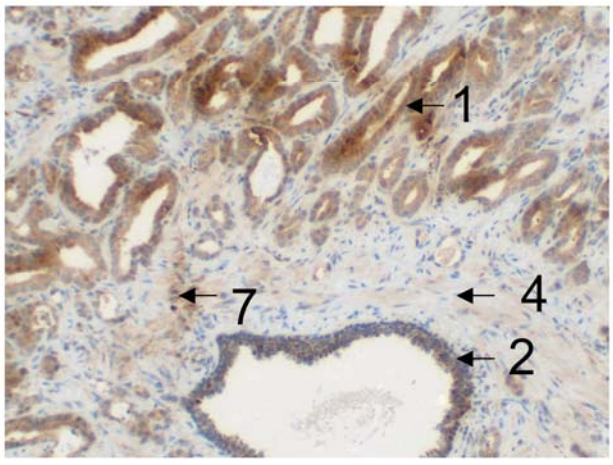

Gleason Pattern 3, Benign Epithelium And Stroma

Figure 2.

A

STC1 Negative control

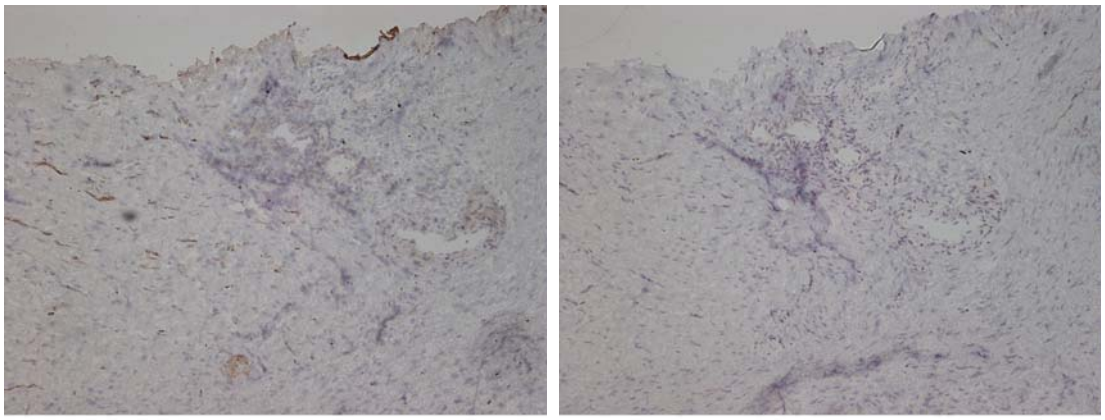

B

STC1 Negative control

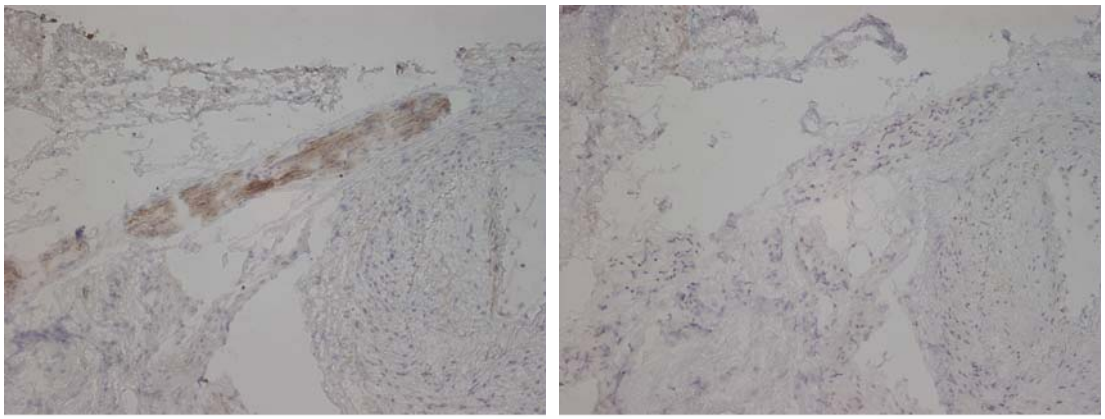

KP-02

Figure 3.

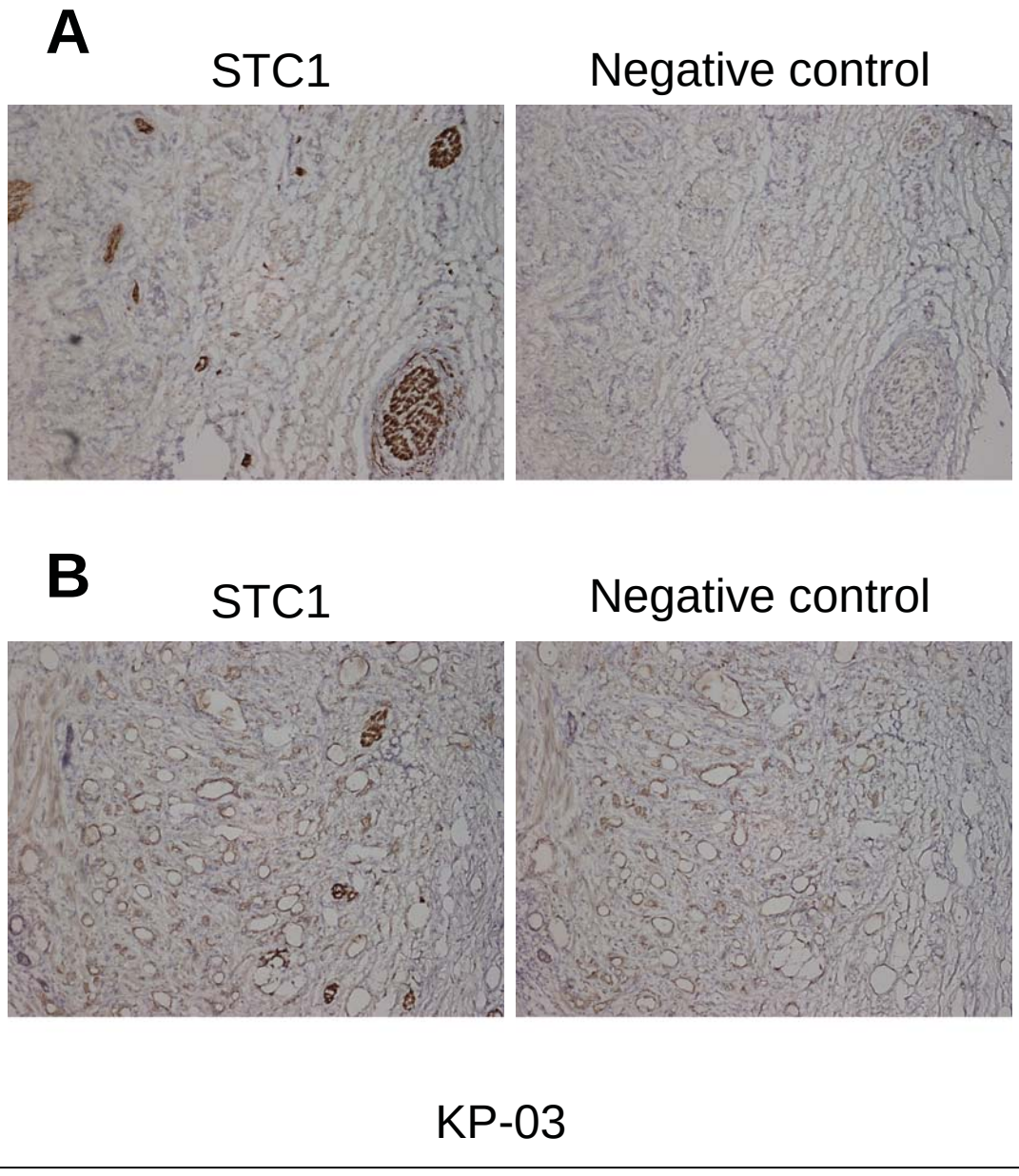

Figure 4.

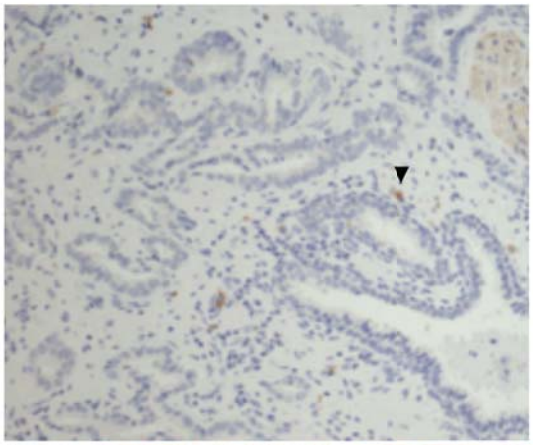

STC1

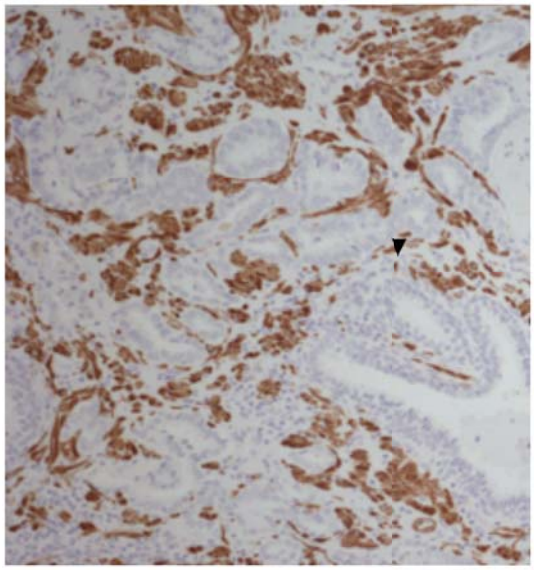

Caldesmon

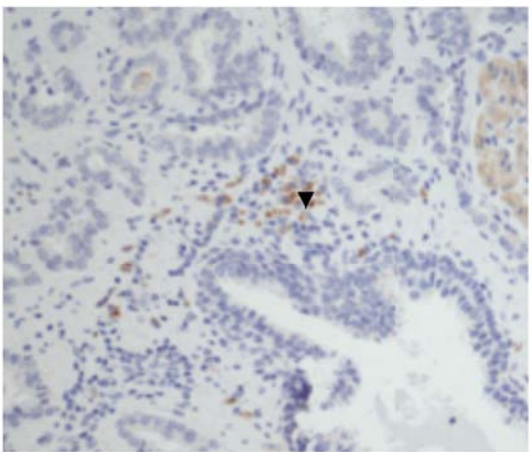

STC1

Figure 5.

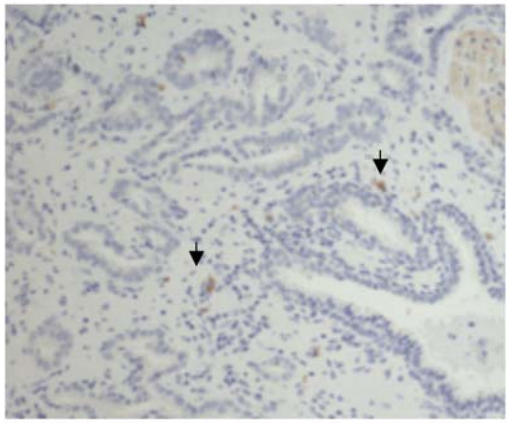

STC1

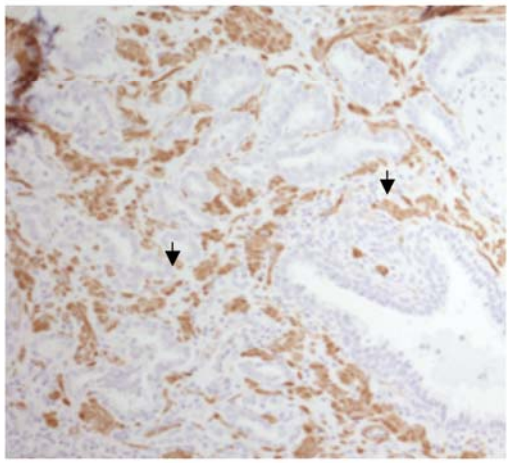

Sm-α-actin

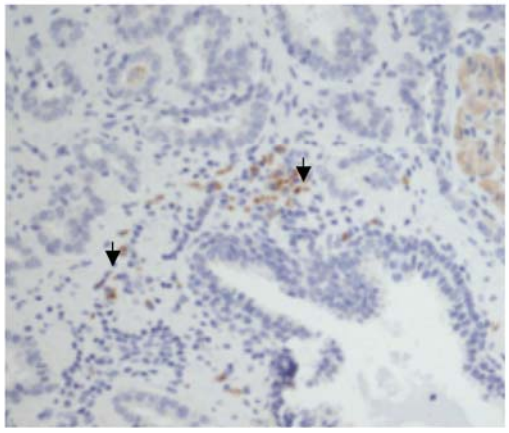

STC1

Figure 6.

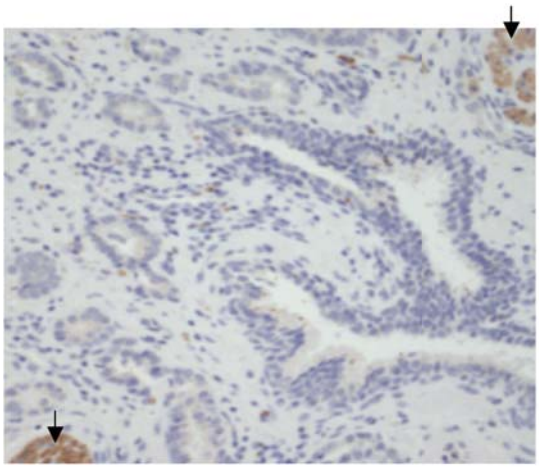

STC1

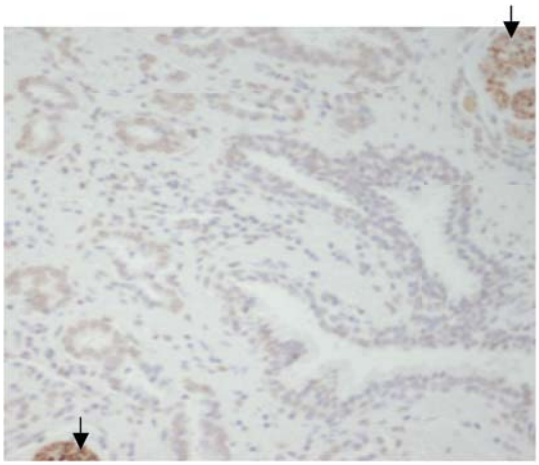

Neurofilament

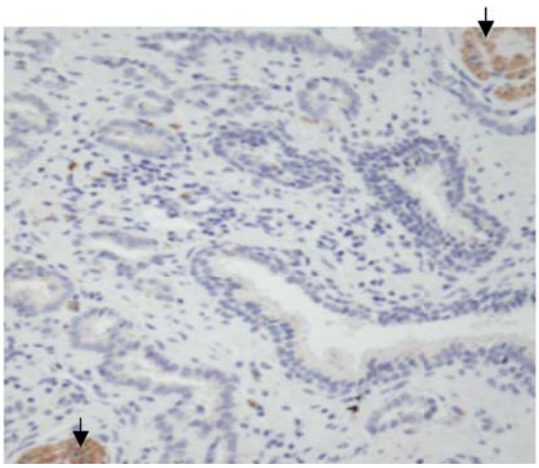

STC1

Figure 7.

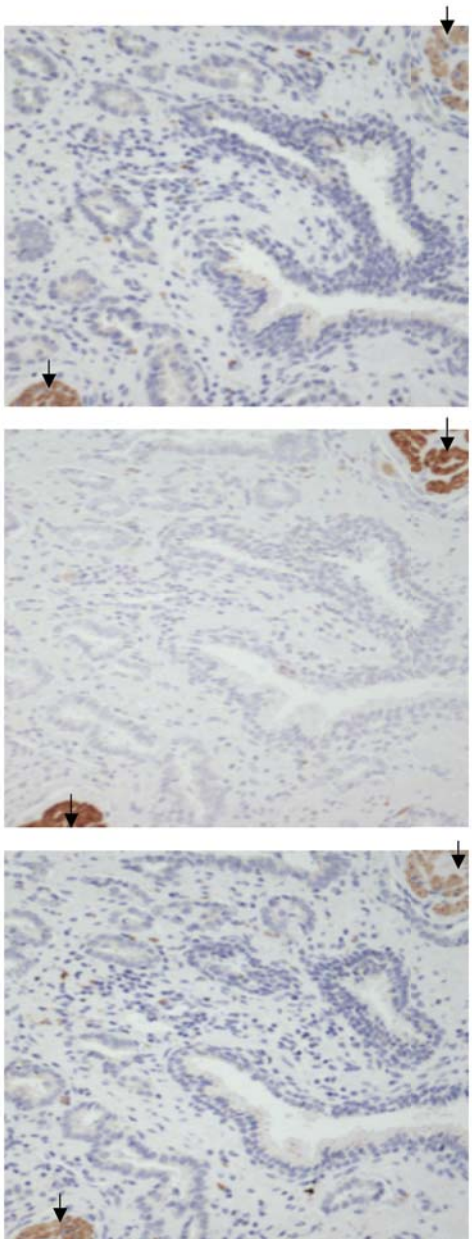

STC1

S100

STC1

Figure 8.

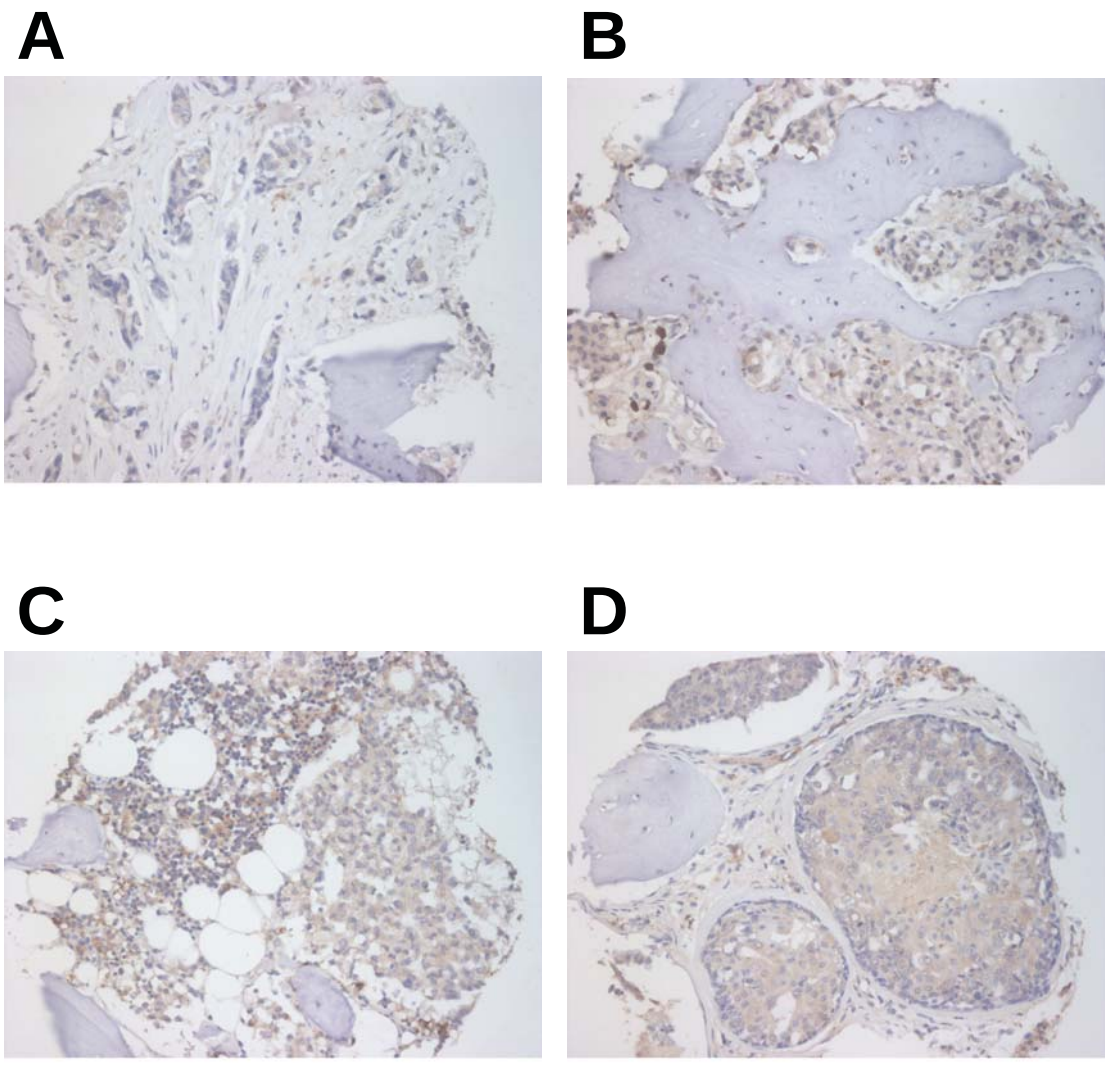

Figure 9.

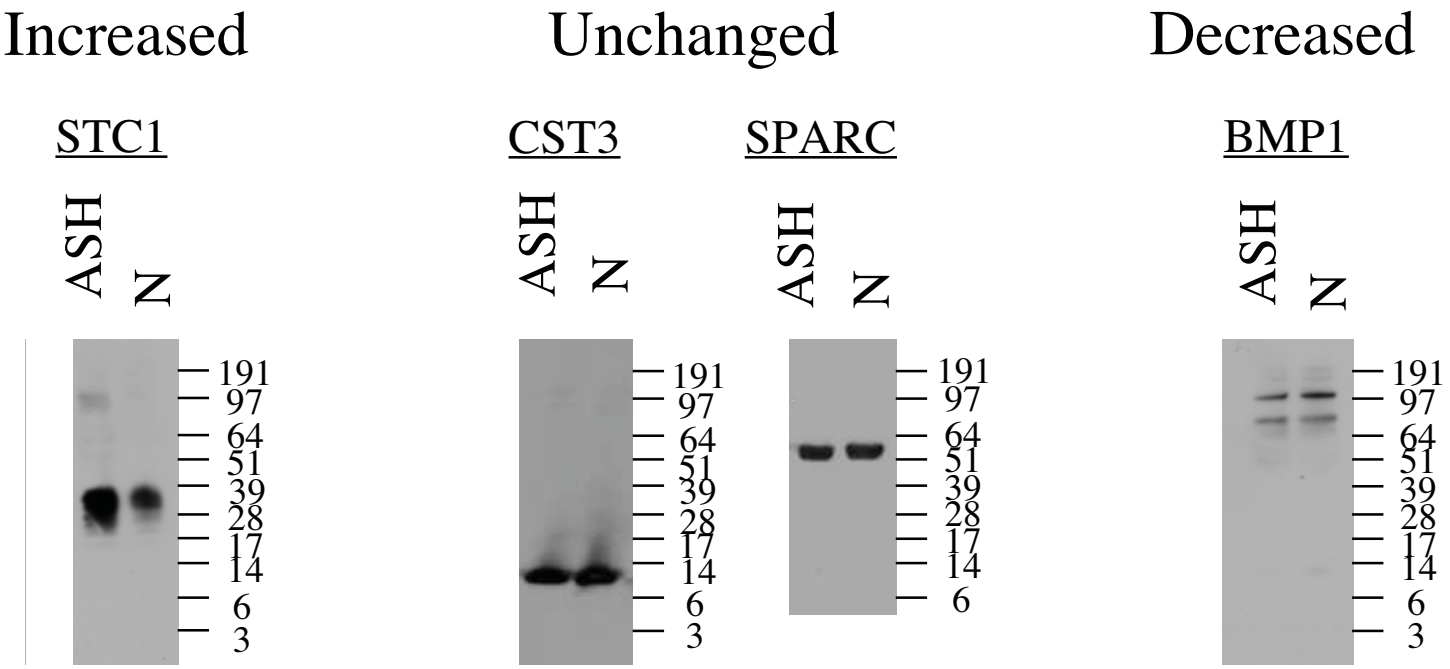
Increased
Unchanged
Decreased
STC1
CST3
SPARC
BMP1
ASH
N
191
97
64
51
39
28
17
14
6
3

Figure 10.

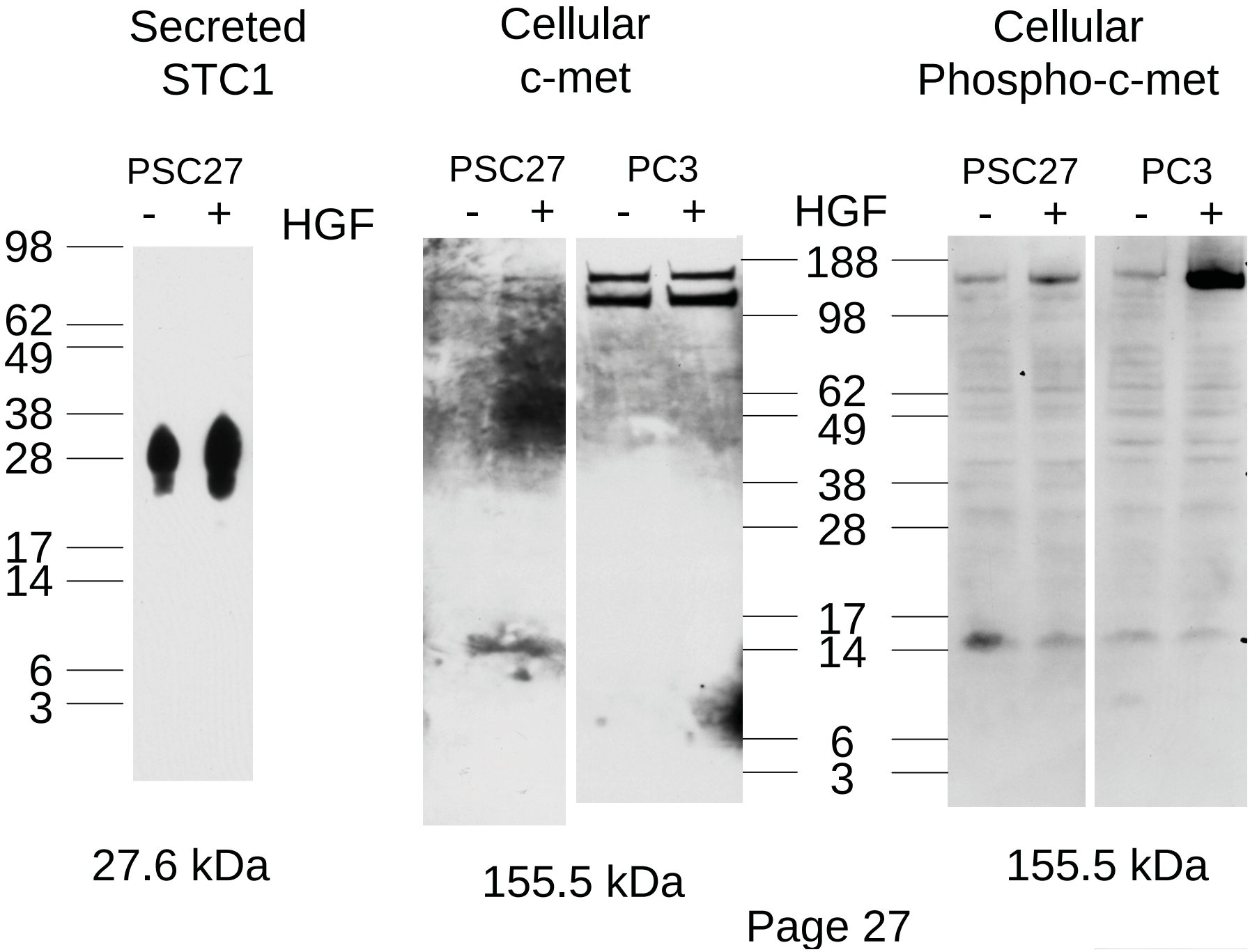
Secreted
STC1
Cellular
c-met
Cellular
Phospho-c-met
PSC27
PSC27
PC3
PSC27
PC3
- + HGF
- + - +
- + HGF
- + - +
98
62
49
38
28
17
14
6
3
188
98
62
49
38
28
17
14
6
3
27.6 kDa
155.5 kDa
155.5 kDa